

## Combined Experimental and Simulation Studies of Cross-Linked Polymer Brushes under Shear

Manjesh K. Singh,<sup>†,□</sup> Chengjun Kang,<sup>†,○</sup> Patrick Ilg,<sup>‡,●</sup> Rowena Crockett,<sup>§</sup> Martin Kröger,<sup>||,●</sup> and Nicholas D. Spencer<sup>\*,†,●</sup>

<sup>†</sup>Laboratory for Surface Science and Technology, Department of Materials, ETH Zurich, CH-8093 Zurich, Switzerland

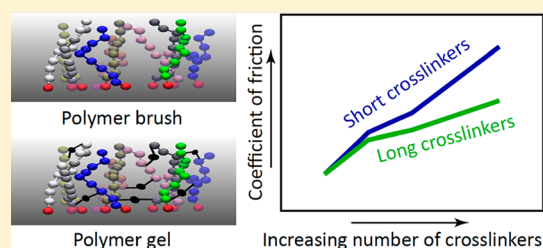
<sup>‡</sup>School of Mathematical, Physical and Computational Sciences, University of Reading, Reading RG6 6AX, United Kingdom

<sup>§</sup>Swiss Federal Laboratories for Materials Science and Technology (EMPA), CH-8600 Dübendorf, Switzerland

<sup>||</sup>Polymer Physics, Department of Materials, ETH Zurich, CH-8093 Zurich, Switzerland

### Supporting Information

**ABSTRACT:** We have studied the effect of cross-linking on the tribological behavior of polymer brushes using a combined experimental and theoretical approach. Tribological and indentation measurements on poly(glycidyl methacrylate) brushes and gels in the presence of dimethylformamide solvent were obtained by means of atomic force microscopy. To complement experiments, we have performed corresponding molecular dynamics (MD) simulations of a generic bead–spring model in the presence of explicit solvent and cross-linkers. Our study shows that cross-linking leads to an increase in friction between polymer brushes and a counter-surface. The coefficient of friction increases with increasing degree of cross-linking and decreases with increasing length of the cross-linker chains. We find that the brush-forming polymer chains in the outer layer play a significant role in reducing friction at the interface.



## 1. INTRODUCTION

Cross-linked polymer brushes are often termed polymer brush gels or simply gels. These polymer gels can swell in either water (hydrogels) or oil (lipogels),<sup>1</sup> making them highly suitable candidates for applications in the fields of drug delivery, pharmaceuticals, tissue engineering, and other biomedical applications.<sup>2–5</sup> Surface-grafted polymer gels can be prepared using two different methods: (i) *in situ* and (ii) *ex situ*. In the *in situ* method, the polymer gels are prepared by cross-linking the chains while growing them from the grafting surface, whereas in the *ex situ* method, polymer gels are prepared by cross-linking the chains in a subsequent step.

Polymer brushes have long been studied using experimental,<sup>6–9</sup> theoretical,<sup>10–14</sup> and modeling<sup>15–21</sup> approaches. Polymer-brush-bearing surfaces exhibit very low friction in a good solvent.<sup>8,22,23</sup> Strong repulsive forces of entropic origin largely prevent the interpenetration of polymer chains grafted on opposing surfaces. Such forces lead to the formation of a thin fluid film between opposing brushes that assists in reducing friction.<sup>7</sup> Studies have been performed to study the effect of different design parameters, such as molecular weight or chain length,<sup>24–27</sup> grafting density,<sup>21,28–31</sup> chain stiffness,<sup>29</sup> and solvent quality<sup>8,32–34</sup> on the tribological behavior of polymer brushes.

There has also been interest in studying the effect of cross-linking on the shear response of polymer brushes.<sup>4,35–42</sup> Lin et al.<sup>43</sup> investigated the effect of cross-linking density and stiffness on the macroscopic behavior of a type 1 collagen gel. It was

found that an increase in the cross-linking density and stiffness (of cross-linkers) leads to an increase in the stiffness of the gel, but the cross-linking density plays the dominant role. The grafted poly[styrene-*b*-(ethylene-*co*-butylene)-*b*-styrene] (SEBS) gel layer showed improved tribological properties (less wear and lower friction coefficient) in comparison to the dry grafted SEBS layer and an *n*-octadecyltrichlorosilane self-assembled monolayer.<sup>44</sup> Recently, the effect of cross-linking was studied using pentaerythritol tetraacrylate as a cross-linking agent for poly(ethylene oxide) gels.<sup>45</sup> It was found that an increase in cross-linker concentration lowers the swelling ratio and increases tensile stress. Cross-linking is known to improve the wear behavior of polymer brushes.<sup>35,46,47</sup> Kobayashi et al.<sup>48</sup> recently showed that the macroscopic friction properties of a diamond-like carbon–silicon (DLC–Si) specimen can be significantly improved by fabrication of an oleophilic cross-linked copolymer brush layer on its surface. Pan et al.<sup>38</sup> studied the friction properties of poly(vinyl alcohol) hydrogels against titanium alloys for biotribological applications under varying loads and shear speeds. They concluded that the effect of load on friction was more significant than that of the speed. Poly(2-hydroxyethyl methacrylate) (PHEMA) hydrogels have been of particular interest to researchers for their potential biotribological

Received: June 26, 2018

Revised: October 24, 2018

Published: December 12, 2018

applications, and studies have been performed for different combinations of substrate and counter-surface.<sup>4,37,49,50</sup> Li et al.<sup>35</sup> studied the effect of degree of cross-linking on the mechanical and tribological behavior of poly(acrylamide) (PAAM) brushes and hydrogels. They found that covalently cross-linked hydrogels display higher Young's moduli and coefficients of friction in comparison with surface-grafted polymer brushes, and the effect was found to increase with the degree of cross-linking. In contrast, Ishikawa et al.<sup>51</sup> compared the effect of mechanical properties and of chemical characteristics (polymer hydration) on tribological behavior of hydrogels via pin-on disk experiments and concluded that the chemical characteristics (e.g., hydration) were the dominant factors. Ohseido et al.<sup>50</sup> studied the effect of the presence of well-defined polymer brushes on gel surfaces. Their study showed that longer poly(sodium 4-styrenesulfonate) (PNaSS) brushes on PHEMA gels exhibit lower friction at low sliding speeds. Dunn et al.<sup>3</sup> explored the distinction between a self-mated "gemini" hydrogel interface and hydrogels sliding against hard, impermeable counter-surfaces and demonstrated that Gemini interfaces have very low friction coefficients, which are independent of sliding speed. On the other hand, hydrogels sliding against rigid impermeable surfaces exhibit higher friction, which is strongly dependent on sliding speed or time in contact. Thus, experimental studies have mainly focused on the role of solvent and effect of degree of cross-linking on the tribological behavior of gels, but to the best of our knowledge the role of the length of cross-linkers has not yet been studied in detail.

We performed complementary experimental and simulation studies to understand the tribological behavior of polymer brushes and gels. We characterized the tribological behavior of poly(glycidyl methacrylate) (PGMA) brushes and gel systems using a colloidal-probe-based lateral force microscopy (LFM) technique. Friction measurements were performed at various applied loads, while maintaining the sliding speed constant. Polymer brushes and gels were modeled using a multibead-spring, coarse-grained molecular-dynamics (MD) simulation technique. We compare the experimental outcome with modeling results to rationalize the effect of cross-linker chains on the frictional behavior of polymer brush gels.

## 2. METHODOLOGY

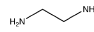
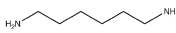
**2.1. Experiment.** **2.1.1. Materials.** Friction experiments were performed on PGMA brushes and gels in dimethylformamide (DMF). The polymers were synthesized using the surface-initiated atom-transfer radical polymerization<sup>52</sup> (SI-ATRP) method on a silicon surface. They are characterized by their mean molecular weight  $M_n = 281.7 \times 10^3$  g/mol and a polydispersity index  $PDI = 1.4$ . The grafting density of the polymer brushes and gels is  $\rho_{\text{expt}} \approx 0.16/\text{nm}^2$ , i.e., 50 times the critical grafting density,<sup>21</sup>  $\rho^* = (\pi R_g^2)^{-1}$ . For details about the estimation of these characteristics for our polymer brushes and gels, see the [Supporting Information](#).

The typical procedures for SI-ATRP of glycidyl methacrylate (GMA) were as follows: 0.141 g (0.9 mmol) of bipyridine (bpy) was dissolved in a mixture of 5 mL of GMA (0.037 mol), 1 mL of H<sub>2</sub>O, and 4 mL of methanol. The mixture underwent four freeze-pump-thaw circles (15 min each) to remove dissolved oxygen. In the next step the mixture was transferred to another flask containing 52.8 mg of CuBr (0.37 mmol) and 4.5 mg of CuBr<sub>2</sub> (0.02 mmol). After stirring for 10 min at room temperature, the mixture was immediately

transferred to freshly prepared, initiator-modified silicon substrates. Polymerization was performed at room temperature for various lengths of time without stirring, after which the silicon substrates were removed from the polymerization solution and sonicated in DMF to remove weakly adsorbed polymer. PGMA brushes were cross-linked by ethane-1,2-diamine or ethane-1,6-diamine in a postmodification manner. Amines can, in principle, react with the epoxypropyl groups in the PGMA in several different ways, since an amine can react with one, two, or even three epoxypropyl groups, and each end of the cross-linker could react with a different number. However, after a series of experiments (detailed in the [Supporting Information](#)), it was determined that, under the conditions used, each end of each cross-linker reacted with a single epoxypropyl group.

Details of polymer brushes and gels used in the tribological experiments are presented in [Table 1](#). Dry thicknesses of

**Table 1. Table Summarizing Experimental Brushes and Gels under Study and in Particular the Cross-Linkers Used in Preparing PGMA Gels**

Materials		Degree of Crosslinking	Dry Thickness
PGMA Brushes		—	93 nm
PGMA gels	 ethane-1,2-diamine Crosslinkers C <sub>2</sub>	5 %	94 nm
		15 %	96 nm
		50 %	102 nm
	 hexane-1,6-diamine Crosslinkers C <sub>6</sub>	3 %	94.5 nm
		18 %	100 nm
		36 %	107 nm

PGMA brushes and gels were measured with a variable-angle spectroscopic ellipsometer (VASE, M-2000F, LOT Oriel GmbH, Darmstadt, Germany) at an incident angle of 70°, using a three-layer model (software WVASE32, LOT Oriel GmbH, Darmstadt, Germany), each sample being measured at three different spots. Cross-linkers of two different lengths were used to prepare PGMA gels with different degrees of cross-linking to facilitate the study of the effect of length and degree of cross-linking on the tribological behavior of the gels. By degree of cross-linking ( $p$ ) we mean

$$p = \frac{2 \times \text{no. of cross-linkers}}{\text{no. of polymer chains} \times \text{deg of polymerization}} \times 100\% \quad (1)$$

**2.1.2. Methods.** Frictional and normal forces between a silica microsphere and PGMA brushes/gels were measured in the presence of DMF solvent by means of atomic force microscopy (AFM). All the measurements were performed using the MFP 3D Instrument (Asylum Inc., Santa Barbara, CA). Asymmetric contact (i.e., brush/gel against bare microsphere) was used to obtain a measurable friction value because friction in symmetric contact (brush-against-brush contact system) is so low as to be at the limit of the resolution of LFM measurements.

The AFM was operated in contact mode, the lateral and normal movements of the cantilever being monitored with a laser beam, reflected off the rear of the cantilever, and detected

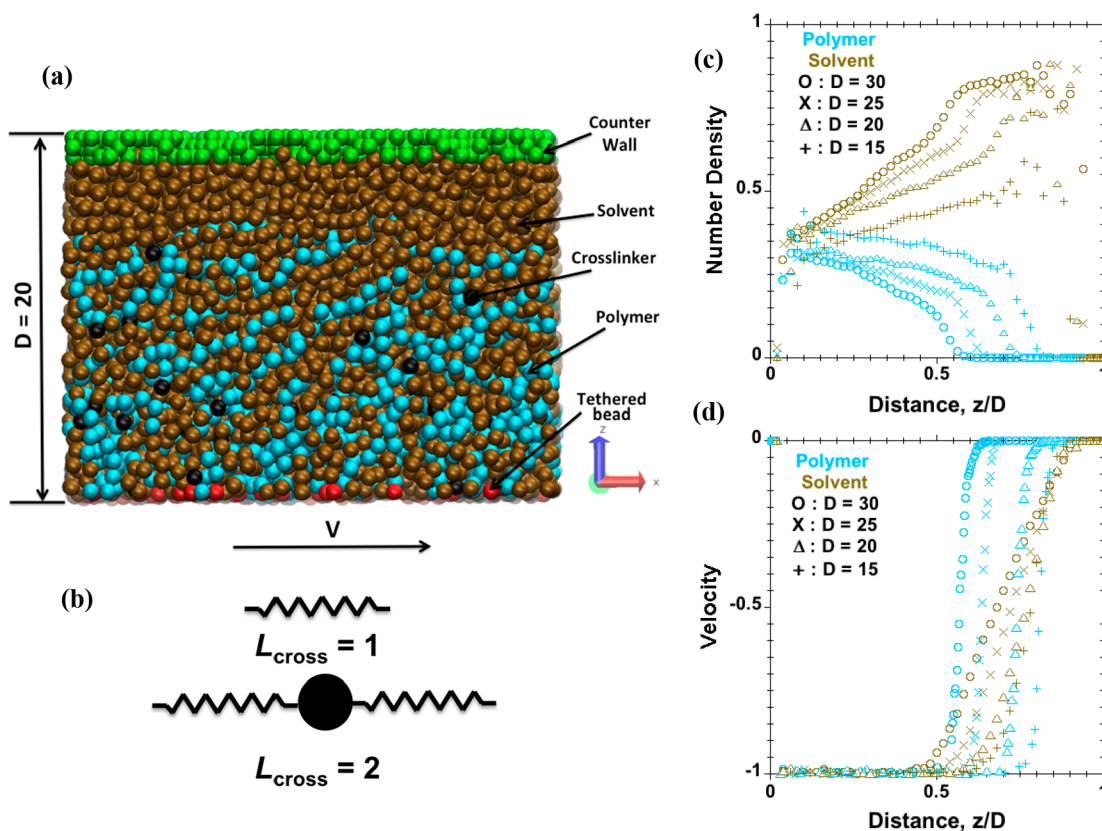


**Figure 1.** Representative information from the model brush-against-wall system with explicit solvent and cross-linkers, subjected to shear. (a) Snapshot, where polymer beads are colored cyan, tethered beads are colored red, solvent beads are colored brown, and cross-linkers ( $L_{\text{cross}} = 2$ ) are colored black. (b) Schematic of cross-linkers of different lengths. (c) Density profiles and (d) velocity profiles versus distance from the grafting surface ( $M = 50$  chains tethered on the grafting surface,  $N = 50$  beads per chain, grafting density  $\rho = 0.075$ , length of cross-linkers  $L_{\text{cross}} = 2$ , and number of cross-linkers  $N_{\text{cross}} = 200$  at velocity  $v = 1$  applied on tethered beads.) All dimensional quantities are given in Lennard-Jones (LJ) units. This particular simulation was performed at very high shear velocity,  $v = 1$ , to achieve a visible amount of alignment, whereas the shear velocity of all subsequent simulations was taken as  $v = 0.001$ .

with a four-quadrant photodiode. These normal and lateral movements of the cantilever can be quantitatively related to the normal and lateral forces acting between the cantilever tip and sample surface if the stiffness of the cantilever and sensitivity of the photodetector with respect to the cantilever position in the respective direction are known.

A nondestructive calibration procedure, the thermal noise method,<sup>53</sup> was used to estimate the normal stiffness of the NSC36 (MicroMasch, Tallinn, Estonia) cantilever. Sader's method<sup>54</sup> was used to calibrate the torsional spring constant of the cantilever. A home-built micromanipulator (attached to a BX 41, Olympus optical microscope, Japan) was used to attach the colloidal particles to a tipless cantilever. In this study, silica microspheres (Kromasil, EKA Chemicals, Sweden) with a diameter,  $d = 14 \mu\text{m}$  (for the friction experiment) or  $d = 10 \mu\text{m}$  (for the indentation experiment) were attached to different tipless cantilevers using a UV-curable glue (NOA 61, Norland optical adhesive, Cranbury, NJ) and were cured overnight using a UV lamp (9 W, Panacol-Elosol, Steinbach, Germany). The lateral sensitivity,  $S_L$ , of the AFM cantilever was estimated using the "test-probe" method<sup>55</sup> as described by Cannara et al. In this method, a colloidal sphere is attached to the cantilever used for calibration, termed the "test cantilever". The "test cantilever" is of similar width and thickness as the cantilever used for measurements or the "target cantilever". The diameter of the colloidal sphere,  $d = 80 \mu\text{m}$ , used for the test cantilever is larger than the width of the cantilever.

For lateral-force measurements, 10 "friction loops" along the same line were acquired at each load. A scanning rate ( $n$ ) of 1.0 Hz and stroke length ( $a$ ) of  $0.5 \mu\text{m}$  were used. Thus, the shear speed applied was calculated as  $v = 2na = 1 \mu\text{m/s}$ . Both the average friction force and the standard deviation were calculated. All the friction experiments were performed at room temperature ( $T = 300 \text{ K}$ ).

**2.2. Simulation.** We investigated an explicit, solvent-based multibead-spring generic coarse-grained model by means of MD simulation. Chains were permanently grafted by one end to a planar surface. To ensure that beads do not cross the grafting surface, an additional 9/3 repulsive wall potential  $U_{\text{wall}}$  was used with cutoff  $z_c = 0.5\sigma$ . Each grafted chain within the polymer brush consisted of  $N$  Lennard-Jones (LJ) beads, linearly interconnected by finite extendable nonlinear elastic (FENE) springs. Each chain was attached to the substrate by one of its ends using an immobile tether bead (red beads in Figure 1). The rest of the beads in each chain were free to move and interact with other polymer beads, the solvent, and the repulsive walls, confining the system to infinitely extended parallel-plate geometry. The solvent was modeled as a simple fluid using spherical beads (brown beads in Figure 1). A solvent molecule consists of one bead that has the same Lennard-Jones diameter as a polymer bead. All the simulations were performed for the brush-against-wall system. The wall was modeled with the help of frozen arrays of repulsive LJ beads. The interaction potential of counter-wall/surface with

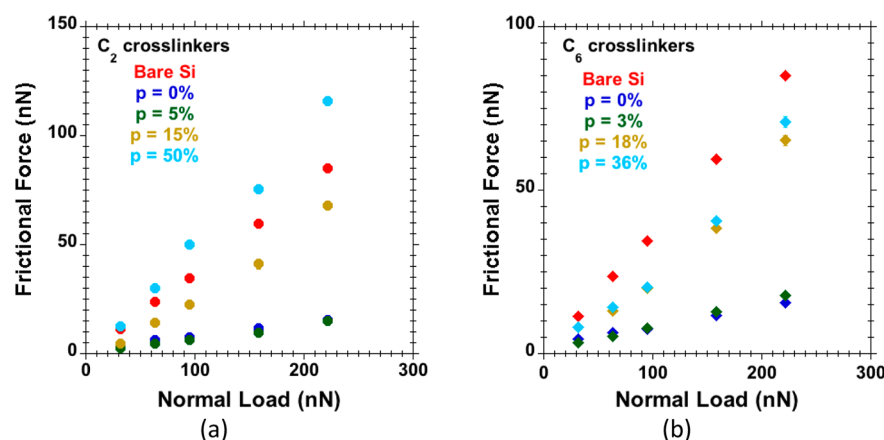


**Figure 2.** Friction force versus normal load for bare silicon surfaces and silicon surfaces bearing PGMA brushes and gels, measured by colloidal-probe lateral force microscopy experiments using a tipless cantilever (0.976 N/m stiffness) with an attached silica sphere of 14  $\mu\text{m}$  diameter. PGMA gels have  $C_2$  cross-linkers with a degree of cross-linking of 5, 15, and 50%. The PGMA gels with  $C_6$  cross-linkers have degrees of cross-linking of 3, 18, and 36%. Experiments were performed at constant speeds of 1  $\mu\text{m/s}$ .

solvent and polymer beads in the simulation is not purely repulsive. We have used a LJ/12–6 potential with cutoff  $R_c = 2.5$  and  $\epsilon = 1.0$ . Periodic boundary conditions were applied only along the lateral direction (along the  $x$  and  $y$  axis of Figure 1a), which coincides with the direction of sliding. To be specific, the explicit solvent model was that employed earlier by Soddemann et al.<sup>56</sup> and Dimitrov et al.<sup>32</sup> The Lennard-Jones (LJ/12–6) potential was truncated at its minimum and shifted to some desired depth (polymer–polymer, solvent–solvent, and polymer–solvent energies  $\epsilon_{pp}$ ,  $\epsilon_{ss}$ , and  $\epsilon_{ps}$ ), continuing from its minimum to zero with a potential having a cosine form and thus providing a potential that both is continuous and has a continuous derivative at the cutoff distance  $r_{c,in}$ . The parameters  $\epsilon_{pp} = \epsilon_{ss} = 0$  and  $\epsilon_{ps} = 0.4$  were chosen to model good solvent conditions in the current work. We have provided details of each potential used in this work in section SVI of the Supporting Information.

The temperature was kept constant by controlling the temperature of all the beads except for tethered and explicit wall beads by explicitly rescaling their individual velocities.<sup>29,57</sup> We have used a profile-unbiased thermostating (PUT) scheme. The velocity profile was calculated by computing the center-of-mass velocity of all beads residing in layers parallel to the grafting surface. The center-of-mass velocity of layers was used to define the “bias velocity”, which was subtracted from the velocities of individual beads to calculate their thermal velocities. These were rescaled to the desired value, and subsequently the bias velocity was added. The temperature was maintained constant at  $T = 1.2$  using a profile-unbiased thermostat as discussed above for all the simulation work in this article.

Details for generating the cross-linked polymer brush were discussed in our previous work.<sup>58</sup> For bonding within cross-linker chains and bonding between cross-linkers and polymer beads as part of the brush, we have used a harmonic bond potential,  $E_H(r) = K_H(r - r_0)^2$ . Here  $K_H$  is the spring coefficient determining the bond stiffness,  $r_0$  is the equilibrium bond length, and  $r$  is the distance between two bonded atoms at any given time. We have used  $K_H = 100$  and  $r_0 = 1$  to model rather stiff cross-linker bonds. The harmonic bond potential we use does not strictly prevent bond crossing, but bond crossing does not occur in practice for the chosen parameters, as

described in the Supporting Information section SV. All simulated quantities reported in this study are given in terms of LJ units.<sup>59</sup> The cross-linked polymer brush system was generated for different numbers of cross-linkers (the number denoted by  $N_{\text{cross}}$ ) with a fixed contour length of cross-linker ( $L_{\text{cross}}$ ) chains, and vice versa. Figure 1b shows the explicit cross-linkers.  $L_{\text{cross}} = 1$  for monomers of different chains bonded by cross-linker, while  $L_{\text{cross}} = 2$  represents a single interior bead that is bonded to two beads in the respective chains to be cross-linked. The degrees of cross-linking ( $p$ ) used in simulation work are  $p = 0, 4, 8,$  and  $16\%$ , as defined in eq 1. For our simulation, we have used LAMMPS (Large-scale Atomic/Molecular Massively Parallel Simulator).<sup>60</sup>

We have performed simulations for the brush-against-wall model system described in Figure 1. We note that the simulations have been performed at fixed separation distances  $D$  (while measuring load), whereas experiments are performed under prescribed normal load (implying a separation distance  $D$ ). The simulations were performed on randomly grafted polymer chains on flat surfaces. The system consists of  $M = 50$  chains on the tethering surface, while each linear chain is composed of  $N = 50$  beads. As mentioned in the section 2.1.1 (see also Supporting Information section SIII), the critical grafting density<sup>21</sup> for such polymer brush is  $\rho^* = (\pi R_g^2)^{-1}$ . We have considered grafting densities well within the brush regime,  $\rho = 0.075$  ( $\sim 7\rho^*$ ). We have not considered additional bending stiffness of chains in the current work; i.e., the simulations were performed on flexible, excluded-volume chains. The total number of beads in the simulation box was such that the number density of beads was maintained at a typical value of  $\sim 0.8$  at each separation between the grafting surface and counter-wall.

### 3. RESULTS AND DISCUSSION

**3.1. PGMA Brushes and Gels in DMF. 3.1.1. Colloidal-Probe Lateral Force Microscopy.** The measured friction force as a function of normal load for PGMA gels with cross-linkers  $C_2$  and  $C_6$  at a shear velocity of 1  $\mu\text{m/s}$  is reported in Figures 2a and 2b, respectively. These results are compared with the corresponding results for a bare silicon surface and PGMA brushes. The experiments were performed in DMF solvent using a tipless cantilever of stiffness 0.976 N/m with a silica colloidal sphere of diameter 14  $\mu\text{m}$  attached to it. The gels had

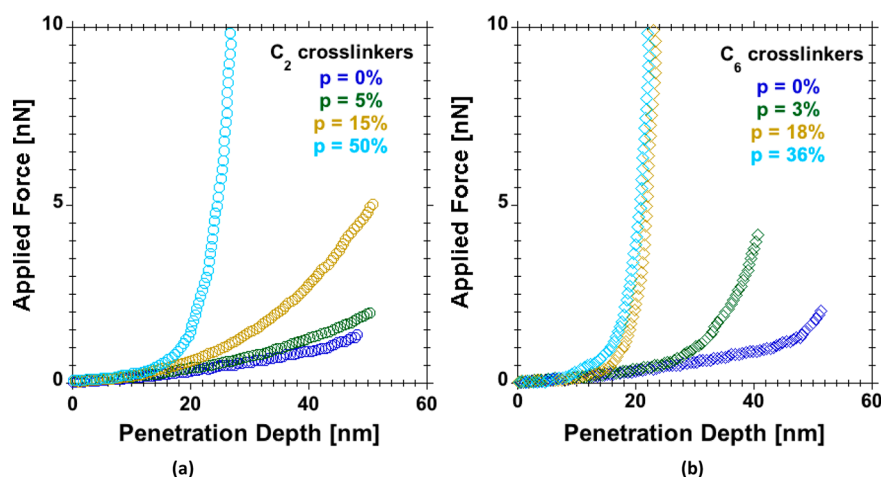


**Figure 3.** Applied force against penetration depth measured by colloidal-probe atomic force microscopy with a  $10\ \mu\text{m}$  silica sphere glued to a tipless cantilever ( $0.6\ \text{N/m}$  stiffness) for (a) PGMA gels with  $C_2$  cross-linkers and (b) PGMA gels with  $C_6$  cross-linkers. % values denote the degree of cross-linking in each system (as for Figure 2).

different degrees of cross-linking. It can be seen that PGMA brushes on silicon surfaces in DMF reduce friction significantly when compared to bare silicon surfaces. The friction force was found to be higher for PGMA gels (i.e., with cross-linking) in comparison to PGMA brushes.

A monotonic increase in friction force is observed upon increasing the degree of cross-linking for gels with  $C_2$  cross-linkers. At 5% degree of cross-linking the friction force is seen to remain close to that for un-cross-linked brushes. At 50% degree of cross-linking, the friction force is higher and even exceeds that of the bare silicon surface. The observed higher friction (in comparison to a bare silicon surface) can be attributed to an increase in contact area between the colloidal sphere and the gel.

Friction is also found to increase with cross-linking degree for gels made with  $C_6$  cross-linkers. At 3% degree of cross-linking, the friction force is only slightly larger than that measured on (non-cross-linked) PGMA brushes. At 18% degree of cross-linking, friction is notably greater than that on (non-cross-linked) PGMA brushes and PGMA gels with 3% degree of cross-linking. With a further increase in degree of cross-linking to 36%, no significant further increase in friction is observed compared to the results obtained with a 18% degree of cross-linking.

Similar experiments were performed at a shear velocity of  $5\ \mu\text{m/s}$  (Supporting Information section SVII). A scanning rate ( $n$ ) of 1.0 Hz and stroke length ( $a$ ) of  $2.5\ \mu\text{m}$  were used. Thus, the shear speed applied was calculated as  $v = 2na = 5\ \mu\text{m/s}$ . The friction coefficient was found to increase with increasing shear speed for all the systems, but the overall trend in terms of the effect of cross-linking was found to be very similar. Polymer brushes and gels in our experiments underwent sliding and were not simply deformed.

The friction force versus normal load curves show a linear relationship. The coefficient of friction can thus be extracted from the slope by linear-regression fitting. The obtained values for the coefficient of friction will be discussed in detail in section 3.3.

**3.1.2. Atomic Force Microscopy (AFM)-Based Nanoindentation.** AFM-based nanoindentation was employed to study the effect of cross-linking on the mechanical behavior of PGMA brushes and gels. The brushes and gels in DMF were

indented with an AFM cantilever bearing a silica sphere of  $10\ \mu\text{m}$  diameter. The applied load (force) against penetration depth is presented in Figure 3.

Figures 3a and 3b show the applied load against indentation depth for different PGMA gels with different cross-linking degrees for  $C_2$  and  $C_6$  cross-linkers, respectively. A change in the slope of the force-versus-depth curve occurs at the depth where the AFM cantilever begins to be noticeably influenced by the substrate; the steep part is caused by a substrate effect (the substrate is close, and the brush appears stiffer). In general, the substrate influence begins to be felt at around 10% indentation of the unperturbed brush height.<sup>61,62</sup> Hence, we can approximate the height of the PGMA brushes and gels by the penetration depth before this sudden change of the indentation force. With  $C_2$  cross-linkers, as the degree of cross-linking increases from 5% to 50%, the substrate effect is shown at a lesser depth, which indicates a decrease in the swelling ratio with increase in degree of cross-linking. The indentation curves for PGMA brushes and PGMA gels with 5% cross-linking are similar, as are the friction forces measured by LFM (cf. Figure 2a). The plausible decrease in swelling ratio with an increase in the degree of cross-linking could explain the increase of friction force: with increasing in degree of cross-linking, there are few brush-forming chains available at the outer film layer, which are responsible for the low-friction behavior in polymer-brush-based lubrication.<sup>9,23,35</sup>

The indentation curves for PGMA gels with  $C_6$  cross-linkers also reflect the tribological behavior of gels observed in LFM experiments. At a degree of cross-linking of 3%, the substrate effect is already significant at penetration depths above 30 nm (implying a decrease in swelling ratio compared to PGMA brushes), which correlates with the increase in coefficient of friction. As the degree of cross-linking is increased to 18%, there is a further decrease in swelling ratio, and an increase in coefficient of friction was observed (Figure 2b). Upon further increasing the degree of cross-linking to 36%, there is no significant change in the indentation behavior anymore; similarly, we did not observe any significant change in the coefficient of friction.

**3.2. MD Simulation.** **3.2.1. Equilibrium Molecular Dynamics Simulation.** We equilibrated the polymer brush/gel against wall system at different separations  $D$  between the

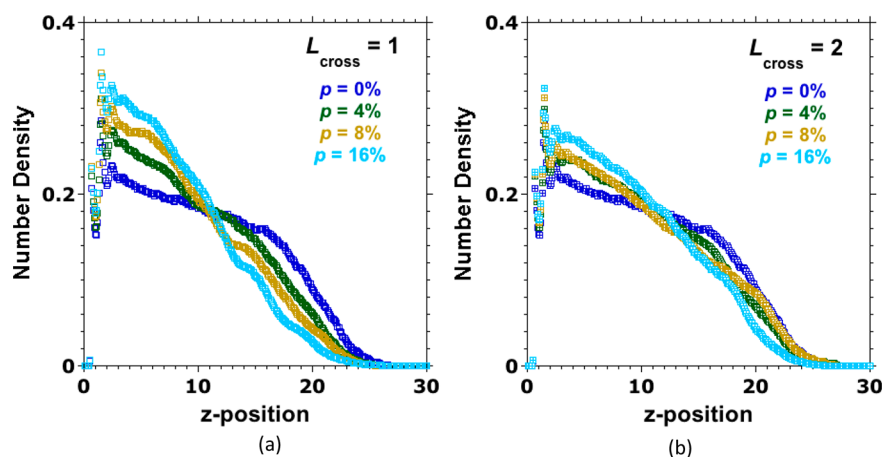


**Figure 4.** Density profiles for polymer brush/gel systems with  $M = 50$ ,  $N = 50$ , and  $\rho = 0.075$  in explicit solvent for a separation distance  $D = 30$ , having (a)  $L_{\text{cross}} = 1$  and (b)  $L_{\text{cross}} = 2$ . Density profiles are shown for different degrees of cross-linking,  $\rho = 0, 4, 8$ , and  $16\%$ .

graft and the counter-wall surface (see Figure 1a). A reduction of separation distance by 1 (LJ unit) was achieved as follows: A number of solvent beads was randomly removed from the system to ensure the same number density 0.8 at the new separation distance. The grafting surface was kept fixed, and the counter-wall was moved toward the grafting surface with a constant velocity  $v = 0.01$  for a duration of  $10^5$  steps at an integration time step  $\Delta t = 0.001$ . At each separation  $D$  between the polymer-chain-bearing surface and counter-wall, the polymer brush/gel system was allowed to equilibrate for  $3 \times 10^6$  time steps ( $10^6$  steps at  $\Delta t = 0.001$  followed by  $2 \times 10^6$  steps at  $\Delta t = 0.0025$ ).

Figure 4 shows the number-density profiles of polymer beads versus the  $z$  position measured from the grafting surface. Upon inspection of the density profiles, the systems with shorter cross-linkers show a decrease in brush height with increasing degree of cross-linking, and more polymer density is accumulated at the grafting surface. There is hence a lower polymer concentration present toward the outer layer of grafted chains to assist in brush-mediated lubrication.<sup>9,63</sup> AFM-based indentation experiments (Figure 3) show that the wet thickness decreases with increasing degree of cross-linking; the simulation observations are in complete agreement with the experiments.

**3.2.2. Nonequilibrium Molecular Dynamics Simulation (NEMD).** The equilibrated systems at different separations ( $D$ ) were used to run nonequilibrium MD (NEMD) simulations. Steady shear was applied by moving the tethered beads with the prescribed velocity, keeping the separation between walls constant during each run of given shear velocity.<sup>20,58</sup> At each separation and velocity, the stress tensor was calculated using the Irving–Kirkwood expression.<sup>59,64</sup>

The NEMD studies were performed at a fixed shear velocity  $v = 0.001$  applied on the tethered beads at different separations between explicit wall and polymer-bearing surface. At each separation, normal and shear stresses acting on the brush and cross-linkers were calculated for different combinations of lengths and numbers of cross-linkers to study the effect of cross-linking on the frictional behavior of model polymer brushes. The simulations were done for  $3 \times 10^7$  integration steps, where data for the first  $10^7$  steps at time step  $\Delta t = 0.002$  were ignored to allow the system to reach steady state. Data for subsequent  $2 \times 10^7$  steps at  $\Delta t = 0.0025$  were recorded and analyzed. Simulations at each separation ( $D$ ) were repeated for

10 different initial configurations of randomly grafted polymer chains, and mean values from these runs are reported with error bars calculated from the corresponding standard deviations.

Figure 5 shows the results on the effect of degree of cross-linking on polymer brushes for different systems having cross-linkers of length  $L_{\text{cross}} = 1$  and  $L_{\text{cross}} = 2$ . In particular, Figures 5a and 5b display normal stress against distance curves for systems with  $L_{\text{cross}} = 1$  and  $L_{\text{cross}} = 2$  cross-linkers, respectively. It can be seen that the normal stress increases as the separation ( $D$ ) between grafting surface and counter-wall surface decreases for all the systems. For systems with  $L_{\text{cross}} = 1$  cross-linkers the normal stress was found to be decreasing with increasing degree of cross-linking at all separations. The decrease in normal stress with the increase in the degree of cross-linking can be explained with the help of the density profile curve (Figure 4a). The brush height decreases with increasing degree of cross-linking; therefore, less deformation is felt in brushes with a higher degree of cross-linking at the same separation between wall and the polymer-bearing surface. This results in a decrease of the normal stress at the same separation with increasing degree of cross-linking.

For the system with  $L_{\text{cross}} = 2$  cross-linkers, normal stress was found to be similar at different degrees of cross-linking and lower in comparison to the un-cross-linked system at all separations. This can be explained with similar density profiles for systems with different degrees of cross-linking. Figures 5c and 5d show the shear stress versus separation distance for systems with  $L_{\text{cross}} = 1$  and  $L_{\text{cross}} = 2$  cross-linkers, respectively. We observe an increase in shear stress as the separation  $D$  between grafting surface and counter-wall surface decreases for all the systems. We also notice an increase in shear stress with increasing degree of cross-linking at all separations. This increase in shear stress is found to be quite similar for  $L_{\text{cross}} = 1$  and  $L_{\text{cross}} = 2$ . Figures 5e and 5f show a parametric plot of shear against normal stress for different separation distances  $D$  for systems with  $L_{\text{cross}} = 1$  and  $L_{\text{cross}} = 2$  cross-linkers, respectively. The shear stress for all the cross-linked systems is found to be higher compared to that of the un-cross-linked system at a given normal stress. We also find an increase in shear stresses with increasing degree of cross-linking at all normal stresses for systems with  $L_{\text{cross}} = 1$  and  $L_{\text{cross}} = 2$  cross-linkers. These observations can be rationalized as follows: Cross-linking leads to an interdependent motion of cross-linked grafted chains

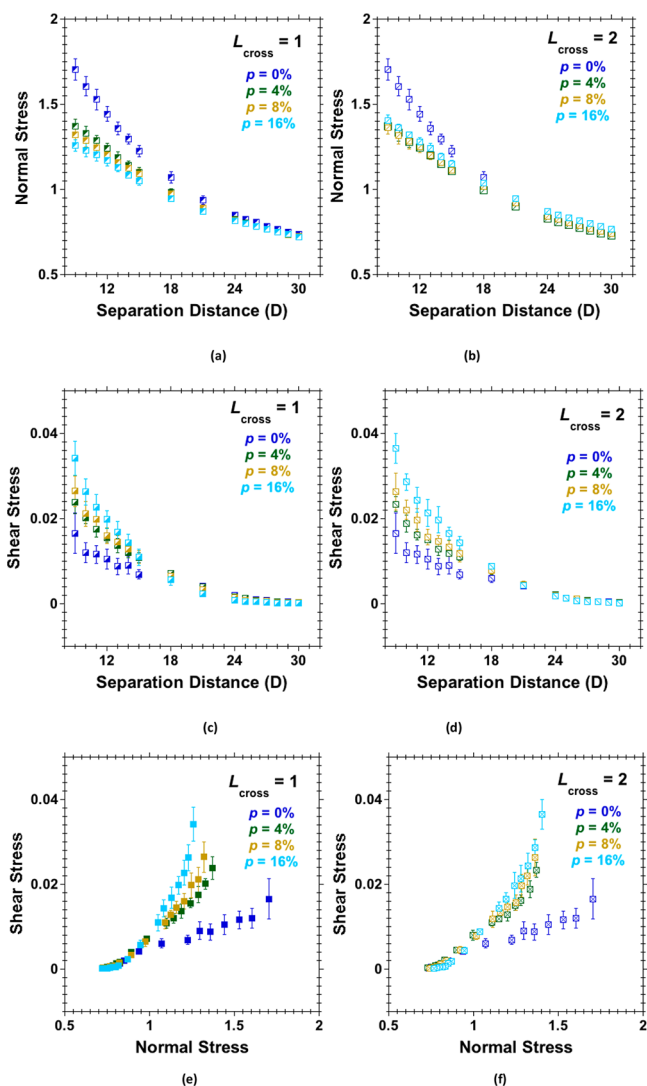


**Figure 5.** Simulated (NEMD) systems with  $M = 50$ ,  $N = 50$ , and  $\rho = 0.075$  in explicit solvent having different degrees of cross-linking,  $p = 0, 4, 8$ , and  $16\%$ : (a, b) normal stress against separation, (c, d) shear stress against separation, and (e, f) shear stress against normal stress each for systems having cross-linkers of length  $L_{\text{cross}} = 1$  and  $L_{\text{cross}} = 2$ , respectively.

under shear, resulting in an increase in the shear stress for all the cross-linked systems when compared to the un-cross-linked polymer brush systems. Under shear, the un-cross-linked systems are deformed more easily than a cross-linked network of polymer brushes.<sup>36</sup> The increase in the degree of cross-linking leads to more chains moving interdependently under shear. We therefore find an increase in friction upon increasing the degree of cross-linking.

**3.3. Comparison between Simulation and Experimental Results.** We are now in a position to attempt a qualitative comparison of the experimental and simulation results. We compare these studies in terms of the coefficient of friction (CoF), which is a frequently used quantity to characterize the tribological behavior of surfaces (Figure 6). To compare flow conditions between experiment and simulation, the dimensionless Weissenberg number ( $Wi = \dot{\gamma}\tau_{\text{Rex}}$  with shear rate  $\dot{\gamma}$  and relaxation time  $\tau_{\text{Rex}}$ ) is typically used. Under the experimental and simulation conditions used in our study,  $Wi$  numbers have comparable values, as demonstrated in the section SIV of the Supporting Information. Our simulations and experiments are located in the boundary-lubrication regime. Friction forces arise due to the interactions among wall, solvent, and polymer beads. We have calculated the coefficient of friction from the slope of the friction force against normal force. Thus, the presented results for the coefficient of friction are unaffected by adhesion between wall and polymer brush. The interaction potential between wall and polymer beads in the simulation is not purely repulsive as mentioned already (section 2.2). It is important to note that the overall interaction between brush and wall can be considered repulsive. There is an attractive van der Waals force present between the brush and wall, which reduces the overall repulsion, but it does not lead to an overall attractive interaction. The van der Waals interactions between polymer brushes and surfaces are considered as “bridging forces” and can be specific or nonspecific. Israelachvili<sup>65</sup> explained in detail various attractive “intersegment”, “bridging”, and “depletion” forces acting between polymers and counter-surfaces. Under suitable conditions, “bridging forces” can lead to an overall attractive force.

For the experiments, a straight line was fitted to the friction-force-versus-normal-load curve in Figure 2. The coefficient of

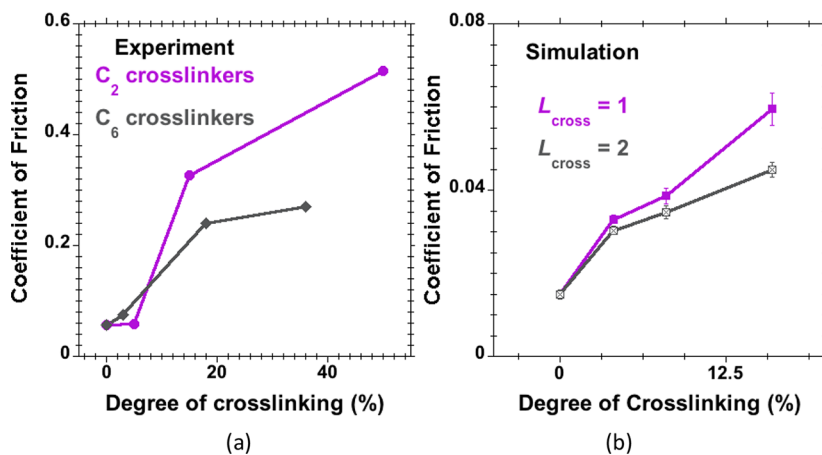


**Figure 6.** Coefficient of friction against degree of cross-linking for (a) experimental results for systems with cross-linkers  $C_2$  (brown lines) and  $C_6$  (gray lines) at a shear speed of  $1 \mu\text{m/s}$  and (b) simulation results for systems with  $M = 50$  chains of length  $N = 50$  for different lengths of cross-linkers,  $L_{\text{cross}} = 1$  (pink lines) and  $L_{\text{cross}} = 2$  (gray lines) at a shear speed,  $\nu = 0.001$  for a brush-against-wall system.

friction is defined by the corresponding slope. Figure 6a shows the resulting CoF as a function of the degree of cross-linking measured by lateral force microscopy at a shear speed of  $v = 1 \mu\text{m/s}$  for different lengths of cross-linkers. We see an increase in friction force with speed for both cross-linking lengths studied here, which translates into an increase in CoF (not shown). We also find an increase in CoF with increasing degree of cross-linking (similar to ref 35) for both cross-linker lengths studied, while the CoF does not change significantly beyond a degree of cross-linking of 18% for  $C_6$  cross-linkers. The coefficient of friction was found to be similar for  $C_2$  and  $C_6$  cross-linkers for lower degrees of cross-linking. At a higher degree of cross-linking, the friction was found to be lower for the gel with longer cross-linkers.

For the simulations, the coefficient of friction was estimated from the slope of the shear-stress-versus-normal-stress curves from the initiation of deformation ( $D < 24$ ) of polymer brushes and gels. The shear-stress-versus-normal-stress curve in this regime is predominantly linear, and a linear curve was fitted taking into account the error at each point in the curve.<sup>66</sup> Figure 6b shows the coefficient of friction versus the degree of cross-linking for different lengths of cross-linkers, as obtained from our simulations. In qualitative agreement with the experiments, the CoF for all the cross-linked systems is found to be higher than that of the un-cross-linked system. The coefficient of friction was also found to increase with the degree of cross-linking for systems having different lengths of cross-linkers in a very similar manner as observed in the experiments. Similar observations were made in the experimental results of Li et al.<sup>35</sup> where the coefficient of friction was found to increase with increasing cross-linker content in PAAm hydrogel brushes.

At a sufficiently high degree of cross-linking, experiments and simulations both show that shorter cross-linker lengths lead to larger values of the CoF. This effect vanishes or is unclear at low degrees of cross-linking. The cross-linkers tend to restrict the configurational space for the chains, so that energetic effects become more relevant. This effect increases with decreasing cross-linker length and increasing degree of cross-linking. In the presence of cross-linkers, the brush thus adopts a more compact density profile (Figure 4), which tends to resist sliding. As a result, the coefficient of friction increases with increasing degree of cross-linking.

#### 4. CONCLUSIONS

Experimental and simulation studies were performed to clarify the effect of cross-linking on the tribological behavior of polymer brushes. The tribological experiments on PGMA brushes and gels in DMF solvent were performed against silica microspheres using the LFM technique. The PGMA brushes showed a remarkable decrease in friction forces when compared to bare silicon surfaces. We also observed a general increase in friction with cross-linking for PGMA brushes in DMF. An increase in the coefficient of friction was observed with increasing degree of cross-linking, and a decreasing coefficient of friction was observed with increasing length of cross-linkers beyond a certain degree of cross-linking. AFM-based indentation of PGMA brushes and gels in DMF solvent showed a decrease in their swelling ratio with increasing degree of cross-linking and can very well explain the tribological response of gels at different degrees of cross-linking for different lengths of cross-linkers.

Cross-linked polymer brushes were successfully modeled using the coarse-grained MD technique. The tribological behavior of cross-linked polymer brushes under shear has been qualitatively compared with that of un-cross-linked polymer brushes and also with our experimental data. Simulations were performed at a constant shear velocity at different separations in the presence of explicit solvent beads. Results were presented in the form of shear stress versus normal stress. The coefficients of friction were calculated from the slopes of shear-stress-versus-normal-stress curves. The trends were consistent with the experimental observations: increase in coefficient of friction with increasing cross-linking degree and decrease in coefficient of friction with increasing cross-linker length. We were able to explain these findings with the help of simulated density profiles. As the degree of cross-linking increases, the polymer concentration in the outer layer that can participate in brush-assisted lubrication is reduced. In addition, cross-linked polymer brushes are more resistant to shear, compared to their non-cross-linked counterparts. We did not attempt to match the shear speeds to achieve a better quantitative agreement between experiments and simulations. Rather, the present simulations aim to study the underlying effects seen in the experiments on a more qualitative level.

This work can be extended by performing studies over a wider range of degree of cross-linking for various lengths of cross-linkers to gain a better understanding of the influence of the length of cross-linkers on the mechanical behavior of gels under shear.

#### ■ ASSOCIATED CONTENT

##### 📄 Supporting Information

The Supporting Information is available free of charge on the ACS Publications website at DOI: 10.1021/acs.macromol.8b01363.

Estimated characteristics of the experimentally studied polymer brushes, possible reaction routes between cross-linkers and polymer brushes, comparison of graft density between experiment and simulation, estimation of Weissenberg number under experimental and simulation conditions, possibility of bond crossing in harmonic bond used for cross-linking, potentials used in simulation, and friction force against normal load at speed  $5 \mu\text{m/s}$  (PDF)

#### ■ AUTHOR INFORMATION

##### Corresponding Author

\*E-mail: [nspencer@ethz.ch](mailto:nspencer@ethz.ch).

##### ORCID

Manjesh K. Singh: 0000-0002-9156-3495

Patrick Ilg: 0000-0002-7518-5543

Martin Kröger: 0000-0003-1402-6714

Nicholas D. Spencer: 0000-0002-7873-7905

##### Present Addresses

□(M.K.S.) Polymer Theory, Max Planck Institute for Polymer Research, D-55128 Mainz, Germany

○(C.K.) Institute of Chemistry and Biotechnology, Zurich University of Applied Sciences, CH-8820 Wädenswil, Switzerland



## Author Contributions

All authors contributed equally to this work. The draft had been prepared by M.K.S. and subsequently revised by all authors.

## Notes

The authors declare no competing financial interest.

## ACKNOWLEDGMENTS

We gratefully acknowledge funding from the European Research Council (ERC) under the European Union's Horizon 2020 research and innovation program (grant agreement no. 669562). The authors thank Debashish Mukherji, Tapan Chandra Adhyapak, and Robinson Cortes-Huerto from MPIP Mainz for a critical reading of the manuscript.

## REFERENCES

- (1) Richtering, W.; Saunders, B. R. Gel Architectures and Their Complexity. *Soft Matter* **2014**, *10* (21), 3695–16.
- (2) Blum, M. M.; Ovaert, T. C. Investigation of Friction and Surface Degradation of Innovative Boundary Lubricant Functionalized Hydrogel Material for Use as Artificial Articular Cartilage. *Wear* **2013**, *301* (1–2), 201–209.
- (3) Dunn, A. C.; Sawyer, W. G.; Angelini, T. E. Gemini Interfaces in Aqueous Lubrication with Hydrogels. *Tribol. Lett.* **2014**, *54* (1), 59–66.
- (4) Freeman, M. E.; Furey, M. J.; Love, B. J.; Hampton, J. M. Friction, Wear, and Lubrication of Hydrogels as Synthetic Articular Cartilage. *Wear* **2000**, *241* (2), 129–135.
- (5) De Giglio, E.; Cafagna, D.; Giangregorio, M.; Domingos, M.; Mattioli-Belmonte, M.; Cometa, S. PHEMA-Based Thin Hydrogel Films for Biomedical Applications. *J. Bioact. Compat. Polym.* **2011**, *26* (4), 420–434.
- (6) Raviv, U.; Klein, J. Adhesion, Friction, and Lubrication Between Polymer-Bearing Surfaces. In *Polymer Science: A Comprehensive Reference*; Elsevier: 2012; pp 607–628.
- (7) Klein, J.; Perahia, D.; Warburg, S. Forces Between Polymer-Bearing Surfaces Undergoing Shear. *Nature* **1991**, *352*, 143–145.
- (8) Nalam, P. C.; Ramakrishna, S. N.; Espinosa-Marzal, R. M.; Spencer, N. D. Exploring Lubrication Regimes at the Nanoscale: Nanotribological Characterization of Silica and Polymer Brushes in Viscous Solvents. *Langmuir* **2013**, *29* (32), 10149–10158.
- (9) Lee, S.; Spencer, N. D. Sweet, Hairy, Soft, and Slippery. *Science* **2008**, *319* (5863), 575–576.
- (10) Alexander, S. Adsorption of Chain Molecules with a Polar Head a Scaling Description. *J. Phys.* **1977**, *38* (8), 983–987.
- (11) De Gennes, P. G. Conformations of Polymers Attached to an Interface. *Macromolecules* **1980**, *13* (5), 1069–1075.
- (12) Milner, S. T.; Witten, T. A.; Cates, M. E. Theory of the Grafted Polymer Brush. *Macromolecules* **1988**, *21* (8), 2610–2619.
- (13) Zhulina, Y. B.; Pryamitsyn, V. A.; Borisov, O. V. Structure and Conformational Transitions in Grafted Polymer Chain Layers. A New Theory. *Polym. Sci. U. S. S. R.* **1989**, *31* (1), 205–216.
- (14) Semenov, A. N. Contribution to the Theory of Microphase Layering in Block-Copolymer Melts. *Zh. Eksp. Teor. Fiz.* **1985**, *25* (17), 1120–1121.
- (15) Kreer, T. Polymer-Brush Lubrication: a Review of Recent Theoretical Advances. *Soft Matter* **2016**, *12* (15), 3479–3501.
- (16) Grest, G. S. Computer Simulations of Shear and Friction Between Polymer Brushes. *Curr. Opin. Colloid Interface Sci.* **1997**, *2* (3), 271–277.
- (17) Hoy, R. S.; Grest, G. S. Entanglements of an End-Grafted Polymer Brush in a Polymeric Matrix. *Macromolecules* **2007**, *40* (23), 8389–8395.
- (18) Grest, G. Interfacial Sliding of Polymer Brushes: a Molecular Dynamics Simulation. *Phys. Rev. Lett.* **1996**, *76* (26), 4979–4982.
- (19) Murat, M.; Grest, G. S. Molecular Dynamics Simulations of the Force Between a Polymer Brush and an AFM Tip. *Macromolecules* **1996**, *29* (25), 8282–8284.
- (20) Singh, M. K.; Ilg, P.; Espinosa-Marzal, R. M.; Kröger, M.; Spencer, N. D. Polymer Brushes Under Shear: Molecular Dynamics Simulations Compared to Experiments. *Langmuir* **2015**, *31* (16), 4798–4805.
- (21) Galuschko, A.; Spirin, L.; Kreer, T.; Johner, A.; Pastorino, C.; Wittmer, J.; Baschnagel, J. Frictional Forces Between Strongly Compressed, Nonentangled Polymer Brushes: Molecular Dynamics Simulations and Scaling Theory. *Langmuir* **2010**, *26* (9), 6418–6429.
- (22) Irfachsyad, D.; Tildesley, D.; Malfreyt, P. Dissipative Particle Dynamics Simulation of Grafted Polymer Brushes Under Shear. *Phys. Chem. Chem. Phys.* **2002**, *4* (13), 3008–3015.
- (23) Chen, M.; Briscoe, W. H.; Armes, S. P.; Klein, J. Lubrication at Physiological Pressures by Polyzwitterionic Brushes. *Science* **2009**, *323* (5922), 1698–1701.
- (24) Goicochea, A. G.; Mayoral, E.; Klapp, J.; Pastorino, C. Nanotribology of Biopolymer Brushes in Aqueous Solution Using Dissipative Particle Dynamics Simulations: an Application to PEG Covered Liposomes in a Theta Solvent. *Soft Matter* **2014**, *10* (1), 166–174.
- (25) Zhang, Z.; Morse, A. J.; Armes, S. P.; Lewis, A. L.; Geoghegan, M.; Leggett, G. J. Effect of Brush Thickness and Solvent Composition on the Friction Force Response of Poly(2-(Methacryloyloxy)-Ethylphosphorylcholine) Brushes. *Langmuir* **2011**, *27* (6), 2514–2521.
- (26) McNamee, C. E.; Yamamoto, S.; Higashitani, K. Preparation and Characterization of Pure and Mixed Monolayers of Poly(Ethylene Glycol) Brushes Chemically Adsorbed to Silica Surfaces. *Langmuir* **2007**, *23* (8), 4389–4399.
- (27) Kitano, K.; Inoue, Y.; Matsuno, R.; Takai, M.; Ishihara, K. Nanoscale Evaluation of Lubricity on Well-Defined Polymer Brush Surfaces Using QCM-D and AFM. *Colloids Surf., B* **2009**, *74* (1), 350–357.
- (28) Rosenberg, K. J.; Goren, T.; Crockett, R.; Spencer, N. D. Load-Induced Transitions in the Lubricity of Adsorbed Poly(L-Lysine)-G-Dextran as a Function of Polysaccharide Chain Density. *ACS Appl. Mater. Interfaces* **2011**, *3* (8), 3020–3025.
- (29) Singh, M.; Ilg, P.; Espinosa-Marzal, R.; Spencer, N.; Kröger, M. Influence of Chain Stiffness, Grafting Density and Normal Load on the Tribological and Structural Behavior of Polymer Brushes: a Nonequilibrium-Molecular-Dynamics Study. *Polymers* **2016**, *8* (7), 254.
- (30) Goicochea, A. G.; López-Esparza, R.; Altamirano, M. A. B.; Rivera-Paz, E.; Waldo-Mendoza, M. A.; Pérez, E. Friction Coefficient and Viscosity of Polymer Brushes with and Without Free Polymers as Slip Agents. *J. Mol. Liq.* **2016**, *219*, 368–376.
- (31) Yamamoto, S.; Ejaz, M.; Tsujii, Y.; Fukuda, T. Surface Interaction Forces of Well-Defined, High-Density Polymer Brushes Studied by Atomic Force Microscopy. 2. Effect of Graft Density. *Macromolecules* **2000**, *33*, 5608–5612.
- (32) Dimitrov, D. I.; Milchev, A.; Binder, K. Polymer Brushes in Solvents of Variable Quality: Molecular Dynamics Simulations Using Explicit Solvent. *J. Chem. Phys.* **2007**, *127* (8), 084905.
- (33) Espinosa-Marzal, R. M.; Nalam, P. C.; Bolisetty, S.; Spencer, N. D. Impact of Solvation on Equilibrium Conformation of Polymer Brushes in Solvent Mixtures. *Soft Matter* **2013**, *9* (15), 4045.
- (34) Nomura, A.; Okayasu, K.; Ohno, K.; Fukuda, T.; Tsujii, Y. Lubrication Mechanism of Concentrated Polymer Brushes in Solvents: Effect of Solvent Quality and Thereby Swelling State. *Macromolecules* **2011**, *44* (12), 5013–5019.
- (35) Li, A.; Benetti, E. M.; Tranchida, D.; Clasohm, J. N.; Schönherr, H.; Spencer, N. D. Surface-Grafted, Covalently Cross-Linked Hydrogel Brushes with Tunable Interfacial and Bulk Properties. *Macromolecules* **2011**, *44* (13), 5344–5351.
- (36) Gong, J. P. Friction and Lubrication of Hydrogels? Its Richness and Complexity. *Soft Matter* **2006**, *2*, 544.

- (37) Kim, S. H.; Opdahl, A.; Marmo, C.; Somorjai, G. A. AFM and SFG Studies of pHEMA-Based Hydrogel Contact Lens Surfaces in Saline Solution: Adhesion, Friction, and the Presence of Non-Crosslinked Polymer Chains at the Surface. *Biomaterials* **2002**, *23* (7), 1657–1666.
- (38) Pan, Y.-S.; Xiong, D.-S.; Ma, R.-Y. A Study on the Friction Properties of Poly(Vinyl Alcohol) Hydrogel as Articular Cartilage Against Titanium Alloy. *Wear* **2007**, *262* (7), 1021–1025.
- (39) Gong, J. P.; Higa, M.; Iwasaki, Y.; Katsuyama, Y.; Osada, Y. Friction of Gels. *J. Phys. Chem. B* **1997**, *101* (28), 5487–5489.
- (40) Caravia, L.; Dowson, D.; Fisher, J.; Corkhill, P. H.; Tighe, B. J. Friction of Hydrogel and Polyurethane Elastic Layers When Sliding Against Each Other Under a Mixed Lubrication Regime. *Wear* **1995**, *181*–*183*, 236–240.
- (41) Gong, J. P.; Kurokawa, T.; Narita, T.; Kagata, G.; Osada, Y.; Nishimura, G.; Kinjo, M. Synthesis of Hydrogels with Extremely Low Surface Friction. *J. Am. Chem. Soc.* **2001**, *123* (23), 5582–5583.
- (42) Mamada, K.; Fridrici, V.; Kosukegawa, H.; Kapsa, P.; Ohta, M. Friction Properties of Poly(Vinyl Alcohol) Hydrogel: Effects of Degree of Polymerization and Saponification Value. *Tribol. Lett.* **2011**, *42* (2), 241–251.
- (43) Lin, S.; Gu, L. Influence of Crosslink Density and Stiffness on Mechanical Properties of Type I Collagen Gel. *Materials* **2015**, *8*, 551–560.
- (44) Julthongpiput, D.; Ahn, H.-S.; Kim, D.-I.; Tsukruk, V. V. Tribological Behavior of Grafted Polymer Gel Nanocoatings. *Tribol. Lett.* **2002**, *13* (1), 35–40.
- (45) Wong, R. S. H.; Ashton, M.; Dodou, K. Effect of Crosslinking Agent Concentration on the Properties of Unmedicated Hydrogels. *Pharmaceutics* **2015**, *7* (3), 305–319.
- (46) Kobayashi, M.; Terada, M.; Takahara, A. Polyelectrolyte Brushes: a Novel Stable Lubrication System in Aqueous Conditions. *Faraday Discuss.* **2012**, *156*, 403–410.
- (47) Zhang, Q.; Archer, L. A. Interfacial Friction and Adhesion of Cross-Linked Polymer Thin Films Swollen with Linear Chains. *Langmuir* **2007**, *23* (14), 7562–7570.
- (48) Kobayashi, M.; Kaido, M.; Suzuki, A.; Takahara, A. Tribological Properties of Cross-Linked Oleophilic Polymer Brushes on Diamond-Like Carbon Films. *Polymer* **2016**, *89*, 128–134.
- (49) Bavaresco, V. P.; Zavaglia, C. A. C.; Reis, M. C.; Gomes, J. R. Study on the Tribological Properties of pHEMA Hydrogels for Use in Artificial Articular Cartilage. *Wear* **2008**, *265* (3–4), 269–277.
- (50) Ohsedo, Y.; Takashina, R.; Gong, J. P.; Osada, Y. Surface Friction of Hydrogels with Well-Defined Polyelectrolyte Brushes. *Langmuir* **2004**, *20* (16), 6549–6555.
- (51) Ishikawa, Y.; Hiratsuka, K.-I.; Sasada, T. Role of Water in the Lubrication of Hydrogel. *Wear* **2006**, *261* (5–6), 500–504.
- (52) Huang, X. Y.; Wirth, M. J. Surface-Initiated Radical Polymerization on Porous Silica. *Anal. Chem.* **1997**, *69* (22), 4577–4580.
- (53) Hutter, J. L.; Bechhoefer, J. Calibration of Atomic-Force Microscope Tips. *Rev. Sci. Instrum.* **1993**, *64* (7), 1868–1873.
- (54) Sader, J. E.; Chon, J. W. M.; Mulvaney, P. Calibration of Rectangular Atomic Force Microscope Cantilevers. *Rev. Sci. Instrum.* **1999**, *70* (1), 3967–3969.
- (55) Cannara, R. J.; Eglin, M.; Carpick, R. W. Lateral Force Calibration in Atomic Force Microscopy: A New Lateral Force Calibration Method and General Guidelines for Optimization. *Rev. Sci. Instrum.* **2006**, *77* (5), 053701.
- (56) Soddemann, T.; Dünweg, B.; Kremer, K. A Generic Computer Model for Amphiphilic Systems. *Eur. Phys. J. E: Soft Matter Biol. Phys.* **2001**, *6* (5), 409–419.
- (57) Kröger, M.; Loose, W.; Hess, S. Rheology and Structural Changes of Polymer Melts via Nonequilibrium Molecular Dynamics. *J. Rheol.* **1993**, *37* (6), 1057–1079.
- (58) Singh, M. K.; Ilg, P.; Espinosa-Marzal, R. M.; Kröger, M.; Spencer, N. D. Effect of Crosslinking on the Microtribological Behavior of Model Polymer Brushes. *Tribol. Lett.* **2016**, *63* (2), 1–9.
- (59) Kröger, M. *Models for Polymeric and Anisotropic Liquids*; Springer: Berlin, 2005.
- (60) Plimpton, S. Fast Parallel Algorithms for Short-Range Molecular Dynamics. *J. Comput. Phys.* **1995**, *117* (1), 1–19.
- (61) Espinosa-Marzal, R. M.; Bielecki, R. M.; Spencer, N. D. Understanding the Role of Viscous Solvent Confinement in the Tribological Behavior of Polymer Brushes: a Bioinspired Approach. *Soft Matter* **2013**, *9* (44), 10572.
- (62) Simič, R.; Mathis, C. H.; Spencer, N. D. A Two-Step Method for Rate-Dependent Nano-Indentation of Hydrogels. *Polymer* **2018**, *137*, 276–282.
- (63) Klein, J.; Kumacheva, E.; Mahalu, D.; Perahia, D.; Fetters, L. J. Reduction of Frictional Forces Between Solid Surfaces Bearing Polymer Brushes. *Nature* **1994**, *370* (6491), 634–636.
- (64) Hess, S.; Kröger, M. Elastic and Plastic Behavior of Model Solids. *Techn. Mech.* **2002**, *22*, 79–88.
- (65) Israelachvili, J. N. *Intermolecular and Surface Forces*; Academic Press: London, 1992.
- (66) Press, W. H.; Flannery, B. P.; Teukolsky, S. A.; Vetterling, W. T. *Numerical Recipes in FORTRAN 77*; Cambridge University Press: 1992; Vol. 1.